

- Ed., Plenum Press, New York, 1977, pp 1-27.
- (3) P. Pulay in ref 2, pp 153-185.
- (4) (a) P. Pulay, *Mol. Phys.*, **18**, 473-480 (1970); (b) *ibid.*, **21**, 329-339 (1971); (c) P. Pulay and W. Meyer, *J. Mol. Spectrosc.*, **40**, 59-70 (1971); (d) W. Meyer and P. Pulay, *J. Chem. Phys.*, **56**, 2109-2116 (1972); (e) P. Pulay and W. Meyer, *ibid.*, **57**, 3337-3340 (1972); (f) W. Meyer and P. Pulay, *Theor. Chim. Acta*, **32**, 253-264 (1974); (g) P. Pulay and W. Meyer, *Mol. Phys.*, **27**, 473-490 (1974); (h) W. Sawodny and P. Pulay, *J. Mol. Spectrosc.*, **51**, 135-141 (1974); (i) P. Pulay and F. Török, *J. Mol. Struct.*, **29**, 239-246 (1975); (j) P. Pulay, A. Ruoff, and W. Sawodny, *Mol. Phys.*, **30**, 1123-1131 (1975); (k) K. Molt, W. Sawodny, P. Pulay, and G. Fogarasi, *ibid.*, **32**, 169-176 (1976); (l) P. Botschwina, *Chem. Phys. Lett.*, **29**, 98-101, 580-583 (1974); (m) W. Bleicher and P. Botschwina, *Mol. Phys.*, **30**, 1029-1036 (1974); (n) P. Botschwina, K. Pecul, and H. Preuss, *Z. Naturforsch. A*, **30**, 1015-1017 (1975); (o) P. Botschwina, W. Meyer, and A. Semkow, *Chem. Phys.*, **15**, 25-34 (1976); (p) P. Botschwina, E. Nachbaur, and B. M. Rode, *Chem. Phys. Lett.*, **41**, 486-489 (1976); (q) P. Botschwina, *Mol. Phys.*, **32**, 729-733 (1976); (r) P. Botschwina, K. Srinivasan, and W. Meyer, *ibid.*, **35**, 1177-1181 (1978).
- (5) (a) H. B. Schlegel, S. Wolfe, and F. Bernardi, *J. Chem. Phys.*, **63**, 3632-3638 (1975); (b) *ibid.*, **67**, 4181-4193 (1977); (c) H. B. Schlegel, S. Wolfe, and K. Mislow, *J. Chem. Soc., Chem. Commun.*, 246-247 (1975); (d) H. B. Schlegel, S. Wolfe, and F. Bernardi, *J. Chem. Phys.*, **67**, 4194-4198 (1977); (e) H. B. Schlegel, private communication (ethane, ethylene, formaldehyde, cyclopropane, thioformaldehyde).
- (6) (a) C. E. Blom, P. J. Slingerland, and C. Altona, *Mol. Phys.*, **31**, 1359-1376 (1976); (b) C. E. Blom and C. Altona, *ibid.*, **31**, 1377-1391 (1976); (c) C. E. Blom, L. P. Otto, and C. Altona, *ibid.*, **32**, 1137-1149 (1976); (d) C. E. Blom and C. Altona, *ibid.*, **33**, 875-885 (1977); (e) *ibid.*, **34**, 177-192 (1977); (f) C. E. Blom, B. Altona, and A. Oskam, *ibid.*, **34**, 557-571 (1976); (g) C. E. Blom and A. Müller, *J. Mol. Spectrosc.*, **70**, 449-458 (1978).
- (7) P. Pulay, *Mol. Phys.*, **17**, 197-204 (1969).
- (8) I. M. Mills, *Spec. Period. Rep., Theor. Chem.*, **1**, 110-159 (1974).
- (9) G. Fogarasi, P. Pulay, K. Molt, and W. Sawodny, *Mol. Phys.*, **33**, 1565-1570 (1977).
- (10) (a) F. Török, A. Hegedüs, K. Kósa, and P. Pulay, *J. Mol. Struct.*, **32**, 93-99 (1976); (b) Yu. N. Panchenko, P. Pulay, and F. Török, *ibid.*, **34**, 283-289 (1976); (c) G. Fogarasi and P. Pulay, *ibid.*, **39**, 275-280 (1977).
- (11) P. Pulay, *Theor. Chim. Acta*, **50**, 299-312 (1979).
- (12) (a) W. Meyer, *J. Chem. Phys.*, **64**, 2901-2907 (1976); (b) W. Meyer and P. Pulay, to be published.
- (13) W. Meyer and P. Pulay, MOLPRO Description, München, Stuttgart, 1969.
- (14) I. G. Csizmadia, M. C. Harrison, J. W. Moskowitz, and B. T. Sutcliffe, *Theor. Chim. Acta*, **6**, 191-216 (1966).
- (15) B. Roos and P. Siegbahn, *Theor. Chim. Acta*, **17**, 209-215 (1970).
- (16) W. Kutzelnigg, private communication.
- (17) W. J. Hehre, W. A. Lathan, R. Ditchfield, M. D. Newton, and J. A. Pople, GAUSSIAN 70, Quantum Chemistry Program Exchange, Indiana University, Bloomington, Ind., 1972, Program No. 236.
- (18) R. Ditchfield, W. J. Hehre, and J. A. Pople, *J. Chem. Phys.*, **54**, 724-728 (1971).
- (19) W. J. Hehre, R. Ditchfield, and J. A. Pople, *J. Chem. Phys.*, **56**, 2257-2261 (1972); P. C. Hariharan and J. A. Pople, *Theor. Chim. Acta*, **28**, 213-222 (1973).
- (20) Examples of near-singular internal coordinates are the sum of the three XAX angles in a nearly planar AX<sub>3</sub> molecule, or the dihedral angle of a near-linear XYZU chain.
- (21) J. L. Duncan, *Spectrochim. Acta*, **20**, 1197-1221 (1964).
- (22) G. Simons, R. G. Parr, and J. M. Finlan, *J. Chem. Phys.*, **59**, 3229-3234 (1973); P. F. Fougere and R. K. Nesbet, *ibid.*, **44**, 285-298 (1966).
- (23) J. C. Decius, *J. Chem. Phys.*, **38**, 241-248 (1963).
- (24) L. H. Jones and R. R. Ryan, *J. Chem. Phys.*, **52**, 2003-2004 (1970).
- (25) C. Eckart, *Phys. Rev.*, **47**, 552-558 (1935).
- (26) This method is referred to briefly by M. Dupuis and H. F. King, *J. Chem. Phys.*, **68**, 3998-4004 (1978).
- (27) H. B. Schlegel, private communication.
- (28) J. W. McIver, Jr., and A. Komornicki, *J. Am. Chem. Soc.*, **94**, 2625-2633 (1972).
- (29) P. Pulay and H. F. Schaefer III, to be published.
- (30) P. Botschwina, *Chem. Phys.*, **28**, 231-241 (1978).
- (31) J. W. McIver and A. Komornicki, *Chem. Phys. Lett.*, **10**, 303-306 (1971).
- (32) Both 4-21 and 4-31G results are cited by J. L. Duncan, D. C. McKean, F. Tullini, G. D. Nivellini, and J. Perez Pena, *J. Mol. Spectrosc.*, **69**, 123-140 (1978).
- (33) L. S. Bertell, S. Fitzwater, and W. J. Hehre, *J. Chem. Phys.*, **63**, 4750-4758 (1975).
- (34) L. A. Curtiss and J. A. Pople, *J. Mol. Spectrosc.*, **48**, 413-426 (1973).
- (35) U. Wahlgren, J. Pacansky, and P. S. Bagus, *J. Chem. Phys.*, **63**, 2874-2881 (1975).
- (36) J. Pacansky, U. Wahlgren, and P. S. Bagus, *Theor. Chim. Acta*, **41**, 301-309 (1976).
- (37) G. Fogarasi and P. Pulay, *Acta Chim. Acad. Sci. Hung.*, submitted.
- (38) P. S. Bagus, J. Pacansky, and U. Wahlgren, *J. Chem. Phys.*, **67**, 618-623 (1977).
- (39) P. Pulay, *Acta Chim. Acad. Sci. Hung.*, **52**, 49-56 (1967).

## Theoretical ab Initio SCF Investigation of the Photochemical Behavior of the Three-Membered Rings. 5. Oxaziridine<sup>1</sup>

B. Bigot,\* D. Roux, A. Sevin, and A. Devaquet

Contribution from the Laboratoire de Chimie Organique Théorique,<sup>2</sup>  
Université Pierre et Marie Curie, 4 Place Jussieu, 75230, Paris Cedex 05, France.  
Received November 1, 1978

**Abstract:** In a first step, MO natural correlation concepts are used in order to understand the potential energy curve profile of the ground and first excited states of the oxaziridine system when different reaction paths are simulated. In a second step, the conclusions of this analysis are corroborated by calculating these potential energy curves by an ab initio SCF CI method. On the one hand, the oxaziridine-nitrene transformations are examined in relation with the cis-trans nitrene isomerization which involves the same intermediate. On the other hand, the formamide-oxaziridine isomerization is studied in relation with the nitrene plus formaldehyde formation. The theoretical results afford a rationale for the spin multiplicity selectivity as well as for an understanding of the origins of various stereospecific transformations experimentally observed. Some predictions relative to the influence of substitutions or solvation are reported.

Since the pioneering works of Emmons<sup>3</sup> and Calvin et al.,<sup>4a</sup> it is now clearly established<sup>5</sup> that oxaziridines may intervene as intermediates in the photochemical reactions of nitrenes.<sup>6</sup> Indeed, isolable oxaziridines can be photochemically formed from nitrenes and then thermally isomerized either back to nitrenes or to other products such as amides. Various authors<sup>4b,7</sup> have proved that oxaziridines can also be converted photochemically to amides. It was observed that the last transformation possesses regioselectivity<sup>3,7a,8</sup> and stereospecificity<sup>8</sup> characters, as well as the photochemical transformation which links nitrene and oxaziridine.<sup>9</sup>

In 1965, Tanaka et al.<sup>10</sup> determined that this nitrene photocyclization involves a singlet state while the photochemically induced cis-trans nitrene isomerization involves a triplet state. Lastly, Bjorgo et al.<sup>11</sup> proved that oxaziridine can also isomerize photochemically back to nitrene and that this process is, in some cases, stereospecific.

Notwithstanding the quality and the number of these experimental results and the theoretical works<sup>9b,12</sup> they called forth, no complete understanding of all these monomolecular reactions has been proposed. For example, what are the factors which govern the NO/CO rupture dichotomy, what is the

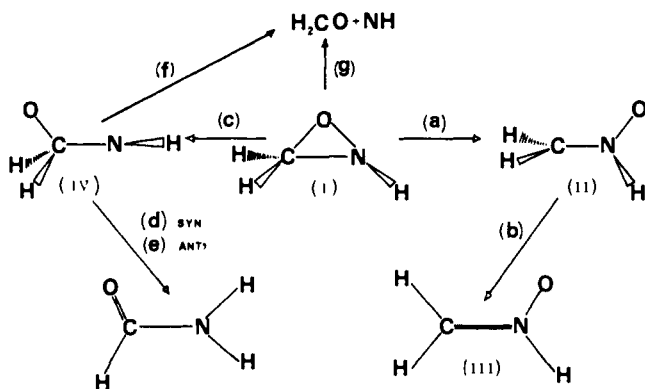


Figure 1. Scheme presenting the different reaction paths for the oxaziridine system presently studied.

origin of the differences found between the triplet and singlet reactivities of nitrones, and what are the factors which explain the stereospecificity in the different processes?

In order to get some new insight on these problems and following our systematic study of the photochemistry of the three-membered rings, we have investigated by theoretical quantum chemistry methods the different reaction paths depicted in Figure 1.

Path (a) corresponds to the oxaziridine (I) ring opening by CO bond rupture. It leads to the structure II, which can, by rotation of the methylene group around the CN bond (path (b)), transform into nitron (III). Path (c) corresponds to the NO bond rupture ring opening. It leads to intermediate IV, which may evolve to amide by migration of the syn (path (d)) or anti (path (e)) hydrogen from the carbon to the nitrogen atom. The syn and anti designations refer to the oxaziridine (I) N-linked hydrogen. By CN bond rupture, intermediate IV cleaves into formaldehyde and nitrene fragments (path (f)). These two species can also be obtained by a simultaneous two-bond scission, directly from oxaziridine (I).

For each of these different paths, the MO and state correlation diagrams have been studied using the natural MO correlation concept.<sup>13a</sup> Let us briefly recall it. To extend the now classical Woodward-Hoffmann<sup>13b</sup> and Longuet-Higgins-Abrahamson<sup>13c</sup> approach to draw qualitative potential energy curves for a chemical reaction path, the natural MO correlation is based on the following procedure. Each MO of the initial system is correlated with the more "alike" MO of the final one. Two MOs are "alike" if—by decreasing importance order—they satisfy the three following conditions. First, in the case when symmetry elements are preserved, they belong to the same irreducible representation of the symmetry group. Second, their phase properties are continuously conserved all along the reaction path. Third, they remain mainly localized on the same fragment. The state diagram is built using the corresponding MO correlation lines. It is only after the last step that the avoided crossings are taken into account leading to the prediction of the potential energy curve (PEC) shapes.

The corresponding potential energy curve calculations of the ground state and low-lying excited states have been performed using an ab initio SCF CI method described elsewhere.<sup>14</sup> It uses the series of GAUSS 70 programs<sup>15</sup> in the minimal STO-3G basis option.<sup>16</sup> The CI segment of our calculations involves the singly and doubly excited configurations obtained by promoting one or two electrons from the six highest occupied to the four lowest unoccupied MOs.

It is quite clear that this procedure suffers some limits. It is, however, more than adequate for our purpose, which is to draw qualitative or semiquantitative conclusions on the PEC shapes based on natural correlation diagram techniques.

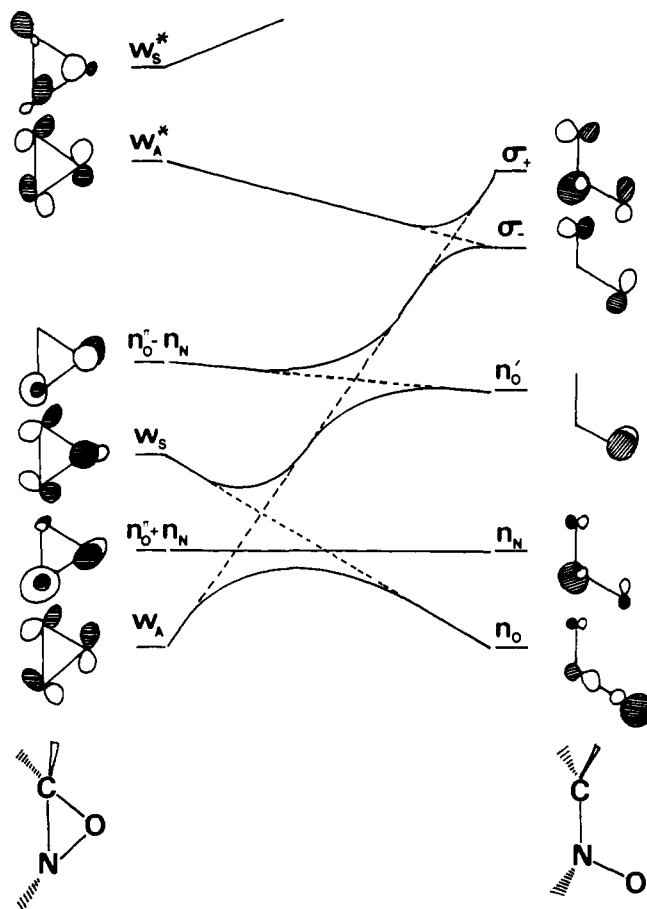


Figure 2. Natural MO correlation diagram in the CO bond rupture of oxaziridine (I) leading to intermediate II. The dashed lines represent the avoided crossings at SCF level.

### Oxaziridine (I) and Nitron (III)

As a starting point in this study, we have adopted for oxaziridine (I) the geometrical parameters reported by Pople et al.<sup>17</sup> Various other calculations<sup>18</sup> on this structure have been performed. The main results are the out-of-plane position of the N-linked hydrogen and the importance of the corresponding inversion barrier (32 kcal/mol). No comparisons can be done with experimental facts since, to our knowledge, nonsubstituted oxaziridine has not been yet isolated.

Let us first describe the different MOs which will be of importance in the discussion. They are represented in Figure 2. By order of increasing energy, we find the four highest occupied MOs:  $W_A$ , so called by analogy with the antisymmetric Walsh orbital of cyclopropane;  $n_O^+ + n_N$ , in-phase combination of the out-of-CNO-plane oxygen and nitrogen lone pairs;  $W_S$ , the symmetric Walsh orbital;  $n_O^- - n_N$ , out-of-phase combination of the preceding lone pairs. Next come the two lowest unoccupied MOs,  $W_A^*$  and  $W_S^*$ , the antibonding Walsh orbitals. Let us now report the nature and energetic position of the first excited states. First one finds the triplet  $n_O^+ + n_N \rightarrow W_A^*$ , which lies at 7.42 eV (166 nm). It is followed by the corresponding singlet at 8.43 eV (146 nm). The next states,  $n_O^- - n_N \rightarrow W_S^*$  (9.25 eV) and  $W_S \rightarrow W_A^*$  (10.18 eV), are triplets. The only experimental comparisons we can make concern substituted oxaziridines whose maximum absorption wavelength is around 250 nm (5 eV).<sup>3,4</sup> It is clear, however, that the calculated values are too high. To improve these results, it would be necessary to use a more extended basis set with polarization functions and a more complete CI than in our procedure. In the present study, we discard these improvements owing to the great cost they would require for the

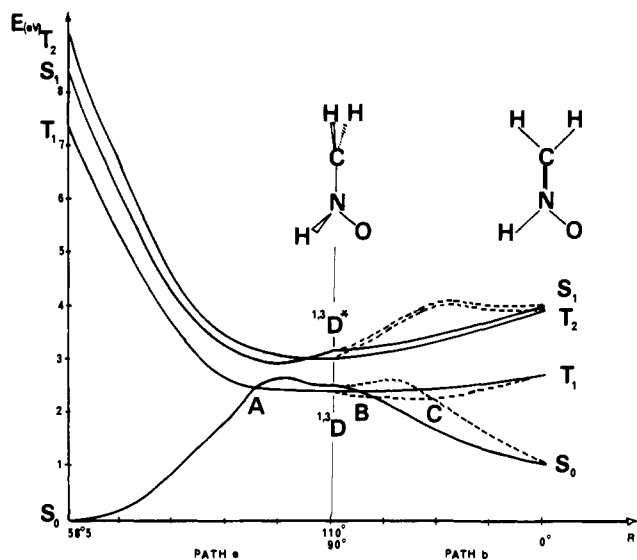


Figure 3. Calculated potential energy curves in path (a) (left part) and path (b) (right part). In path (b), the full lines refer to the syn motion and the dashed lines to the anti motion.  $R$  is a reaction coordinate. It refers to the CNO angle in the left side and to the dihedral angle between the  $\text{CH}_2$  and CNO planes in the right side. In this figure and in Figures 8, 12, and 14, the calculated points are indicated in abscissas.

determination of the PECs, and because we are mainly interested in qualitative rather than in quantitative explanations and predictions. Other works have shown that the present procedure is, however, of chemical significance.<sup>1,13,14</sup>

For the nitron molecule, a complete optimization of the ground-state geometry has been achieved.<sup>19</sup> The main MOs concerned in the present study are, by increasing energy order,  $\pi_1$ , the allylic-type bonding MO, mainly located on the nitrogen atom,  $n_{\text{O}}$  and  $n_{\text{O}'}$ , the two oxygen lone pairs, and  $\pi_2$  and  $\pi_3$ , the two last  $\pi$  allylic type MOs (Figure 5).

The ground state is a singlet state ( $0.90\pi_2^2 - 0.34\pi_2\pi_3$ ) possessing at once radical and ionic character.<sup>20</sup> The next state is the  $\pi_2 \rightarrow \pi_3$  triplet which lies at 1.67 eV (739 nm); it is followed by the  $n_{\text{O}} \rightarrow \pi_3$  triplet-singlet pair (2.86 eV = 433 nm and 2.96 eV = 419 nm, respectively).

Experimentally, substituted nitrones have a maximum absorption wavelength in the range 310–420 nm.<sup>21</sup>

#### Oxaziridine (I)–Nitron (III) Transformation. Paths (a) and (b)

To transform oxaziridine (I) into nitron (III), we can distinguish two typical reaction paths. The first one consists in a direct transformation with simultaneous NO bond rupture-ring opening and methylene-group rotation. The second one is a two-step process. First, the ring is open through NO bond rupture to a CNO angle close to  $110^\circ$ . Then the methylene group rotates from a perpendicular to a CNO in-plane position. The calculations show that the first process requires much more energy than the second one.<sup>22a</sup> We will limit ourselves to study the latter reaction path model.

Let us first consider the structure II. Fixing the CNO angle to an arbitrary value of  $110^\circ$ ,<sup>22b</sup> we have optimized its geometry. The calculations lead to a structure<sup>23</sup> where the N-linked hydrogen is not in the CNO plane, in agreement with semi-empirical calculations<sup>24</sup> previously reported.

**Path (a).** The reaction coordinate is the CNO angle ( $58.5^\circ \rightarrow 110^\circ$ ). All the other parameters are linearly modified. The natural MO correlation diagram (Figure 2, dashed lines) is drawn according to the phase relation and location conservation rules.<sup>13a</sup> At the SCF level, all the crossings are avoided and the full line correlations result. The origin of the  $\sigma^+/\sigma^-$  energy

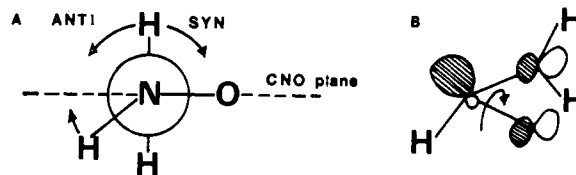


Figure 4. (A) Newman projection of structure II along CN bond illustrating the different syn and anti motion in path (b). (B) Schematic representation of the  $n_{\text{N}}$  MO of the structure II depicting the rotation of the lobe located on the oxygen atom in path (b).

order is similar to that encountered by Hoffmann<sup>25</sup> in the EE open form of cyclopropane for the  $\pi^+/\pi^-$  couple.

Before concluding on the PEC shapes, let us define the lowest states of structure II. The first one is the  $\sigma^- \rightarrow \sigma^+$  triplet. It lies 2.40 eV above the oxaziridine ground state. The next one is a singlet state ( $0.73(\sigma^-)^2 - 0.54(\sigma^- \rightarrow \sigma^+)^2 + 0.30(\sigma^- \rightarrow \sigma^+)$ ), which is a diradical with nonnegligible zwitterionic character. It lies 0.17 eV above the triplet. Let us call them  $^{1,3}\text{D}$  states. At last comes another singlet-triplet pair,  $^{1,3}\text{D}^*$ , corresponding to the  $n_{\text{O}'} \rightarrow \sigma^-$  excitation.

Since there is a HOMO–LUMO crossing at the MO natural correlation level (see Figure 2), two main features may be expected to result<sup>13a</sup> for the PECs at the end of path (a). First, a faint maximum is predicted on the PEC which links oxaziridine ground state to the structure II  $^1\text{D}$  state. Second, faint minima on the  $^{1,3}(n_{\text{O}'}\pi + n_{\text{N}} \rightarrow \text{W}_A^*) \rightarrow ^1\text{D}^*, ^3\text{D}$  PECs are also predicted. The calculated curves (Figure 3, left side) are in correct agreement with these predictions.

**Path (b).** To convert structure II into nitron (III), two reaction paths are possible. Let us define them in relation with the CNO plane. To form III from II, the N-linked hydrogen must move into this plane while the methylene group rotates around the CN bond. Two rotation modes are possible: either the methylene rotation is in the same direction (syn process) or in the inverse direction (anti process) as that of the N-linked hydrogen motion (see Figure 4A).

The calculations show that the syn process corresponds to a MO disrotatory motion and conversely that the anti process corresponds to a MO conrotatory motion. The reason is related to the phase properties of the structure II  $n_{\text{N}}$  orbital. It is the only occupied orbital which possesses a nonnegligible contribution on the three heavy atoms. During the syn or anti process, the oxygen localized lobe moves in the way indicated in Figure 4B in order to preserve its phase relationship with the nitrogen lobe. It follows that the syn process is, this way, a disrotatory motion and conversely that the anti process is a conrotatory motion.

The natural MO correlation diagrams result from these considerations (see Figure 5). A HOMO–LUMO crossing occurs in the anti process, while none appears in the syn process. This crossing is avoided at SCF level, but it has important consequences regarding the PEC shapes.

Indeed, a faint maximum on the structure II  $^1\text{D}$  state–nitron (III) GS PEC must be expected in the anti process while none must appear in the syn process. Conversely a faint minimum must occur on the  $^3\text{D}-^3\pi_2\pi_3$  PEC in the anti process and none in the syn. Now, let us draw the state correlation diagram concerning the  $^{1,3}\text{D}^*$  and  $^{1,3}n_{\text{O}'}/\pi_3$  pairs (Figure 6).

In the syn process they are directly correlated. In the anti process the  $^{1,3}\text{D}^*$  pair correlates with the doubly excited  $^{1,3}(n_{\text{O}'}/\pi_2 \rightarrow \pi_3^2)$  pair and conversely the  $^{1,3}(n_{\text{O}'}/\pi_3)$  pair with the doubly excited  $^{1,3}(n_{\text{O}'}/\sigma^- \rightarrow \sigma_+^2)$  pair (dashed lines). The crossings are avoided and maxima must occur on the PECs.

The calculated curves are in full agreement with these predictions (Figure 3, right side).

From the calculated PECs relative to path (a) and path (b) (syn and anti), the oxaziridine–nitron transformation and the

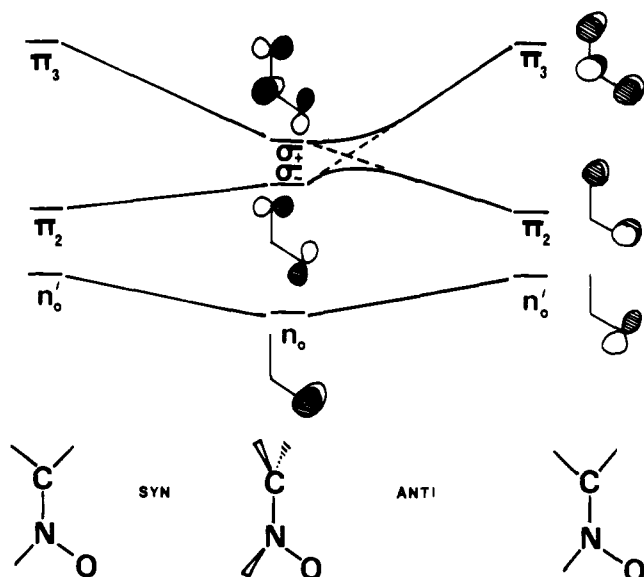


Figure 5. Natural MO correlation diagram in path (b) for the syn and anti motions.

cis-trans isomerization can be analyzed at the same time. Indeed, the last transformation consists, for example, in path (b) syn followed by path (b) (anti) and involves the same structure (II) intermediate.

Let us first consider the oxaziridine reactivity.

Thermally, the oxaziridine (I)-nitronium (III) transformation requires the overcoming of a 2.5-eV (58 kcal/mol) energy barrier. This appears as an upper limit of the real barrier. The difference existing between the syn and anti processes is feeble (5 kcal/mol), but it favors, however, the syn process.

Photochemically, the  $S_1$  state is quite reactive. It leads to the formation of an intermediate whose structure is very near to the structure II. It corresponds to the minimum on the  $S_1$  PEC, which is in a situation of near touching with the  $S_0$  PEC. From this minimum, different decay processes are possible. The first one leads back to oxaziridine GS. It involves a jump from  $S_1$  to  $S_0$  PEC for an opening angle value less than  $100^\circ$ . The second and third ones lead to the nitronium GS through the syn or anti process, respectively, if the ring opening goes more forward. The position of the minimum on the  $S_1$  state and the energy gap between the  $S_1$  and  $S_0$  PECs favor the first two processes: ring reclosure to oxaziridine and syn formation of nitronium.

The  $T_2$  state behaves the same as  $S_1$ , while the  $T_1$  state leads to a different evolution. The latter is also reactive and the system can easily reach the corresponding PEC's minimum region where three crossings with the  $S_0$  PECs occur (points A, B, and C). The most effective intersystem crossings appear to take place in A and C, in the region of the minima previously described for path (a) and path (b)  $T_1$  PECs. The first one (A) leads to ring reclosure to oxaziridine, the second one (C) to the formation of nitronium through an anti process.

Let us now consider the nitronium reactivity.

Thermally the nitronium can transform into oxaziridine after overcoming a barrier of ca. 1.5 eV. The syn process is favored. However, in this case the resulting oxaziridine molecule would possess such an excess of internal energy (ca. 2.5 eV) that, very likely, further reactions would occur, for example, a NO bond rupture leading to formamide (vide infra). Another possibility is cis-trans isomerization, which requires only a little more energy than the preceding oxaziridine formation process. The importance of the calculated barrier (1.55 eV) appears in correct agreement with experimental results.<sup>24</sup>

Photochemically,  $S_1$  is a reactive state leading to structure II through a syn process. It leads to the previously described

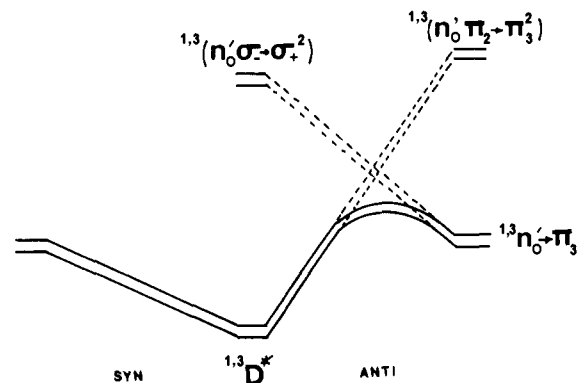


Figure 6. State correlation diagrams resulting from natural MO correlation (Figure 5) in path (b) for the singlet-triplet pair  $D^*$ . The full lines represent the PECs after solving of the avoided crossings.

minimum on the  $S_1$  PEC. The preferential decays give either oxaziridine or the initial nitronium (syn process) (vide supra).  $T_2$  has the same reactivity as  $S_1$ .  $T_1$  is less reactive and it appears that its easiest reactive path is nitronium isomerization. For example, the process begins by a syn nitronium-structure II transformation and ends, via an intersystem crossing at point C, on the PEC of the anti motion. Owing to the quite degenerate position of the  $^3\pi_2\pi_3$  and  $^3D$  states, it seems that the system may hardly reach the point A to lead to oxaziridine by intersystem crossing.

All these results are in correct agreement with the experimental findings. One interesting point is the  $S_1$ - $T_1$  dichotomy in the oxaziridine-nitronium transformation.  $S_1$  leads preferentially to a syn process while  $T_1$  leads to an anti process. However, owing to the great reactivity of the  $S_1$  state, it seems that for observing the  $T_1$  reactivity it would be necessary to populate this state directly by sensitization.

**Path (c).** Path (c) corresponds to the ring opening via NO bond rupture and leads to the open structure IV. Fixing the NCO angle to a value of  $110^\circ$ , all the other geometrical parameters of this structure have been optimized.<sup>26</sup> Let us note that the N-linked hydrogen is very clearly located out of the NCO plane, thus conserving its stereochemical relationship with respect to the carbon substituents. The in-plane position of this hydrogen would lead to the existence of three electrons in the same space region. This situation is very unfavorable.

Let us define the different MOs of the structure IV which will be of main concern in the following discussion. By order of increasing energy, we have  $n_N$ , mainly located on the nitrogen atom and which looks like the lone pair; then the out-of-plane oxygen lone pair  $n_O$  comes and last we find the  $\sigma^+/\sigma^-$  couple, in- and out-of-phase combination of the in-plane lobe located on the ends of the NO broken bond. The first electronic states of structure IV are the singlet and triplet diradicals  $^1,^3D_{\sigma\sigma}$ . They lie 1.41 and 1.47 eV above the oxaziridine GS, respectively. They correspond to the location of one electron at each end of the NO broken bond. Next, we get the  $^1D_{\sigma\pi}$  pair (1.53 and 1.55 eV), quite degenerate with the preceding couple. It corresponds to the promotion of one electron from the  $n_O$  orbital to the  $\sigma^+/\sigma^-$  couple.

Along path (c), the reaction coordinate will be referred to the NCO angle. All the other parameters are linearly modified from the initial structure to the final one.

In the MO natural correlation diagram, no HOMO-LUMO crossing occurs (Figure 7). It follows that the state correlations will be direct and no extremum can be predicted on the PECs. This is confirmed by the calculated curves (Figure 8, left side).

**Paths (d) and (e).** Many works have been devoted to the oxaziridine (I)-formamide (V) transformation and various

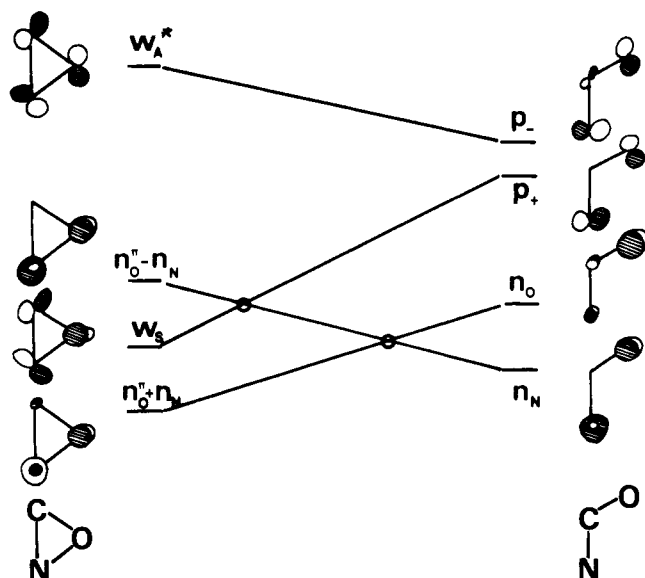


Figure 7. Natural MO correlation diagram in the NO bond rupture (path (c)). The circles represent avoided crossings at SCF level.

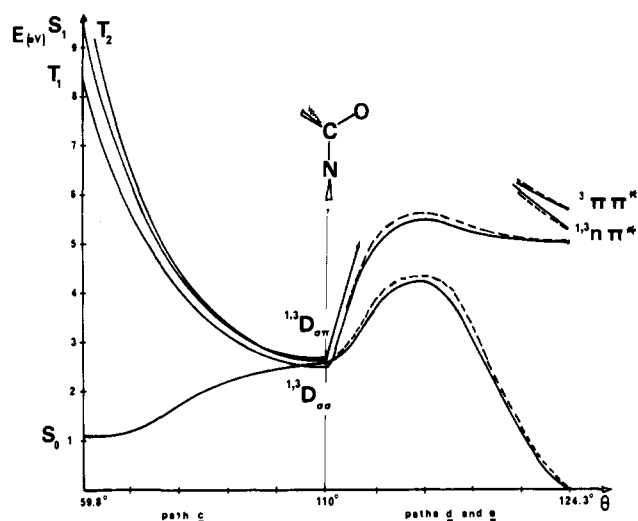


Figure 8. Calculated potential energy curves in path (c) (left part) and paths (d) and (e) (right part). On the right part, the full lines refer to path (d) and the dashed lines to path (e). Only the two lowest state PECs are represented. The reaction coordinate  $\theta$  refers to the NCO angle.

tentative rationalizations have been proposed.<sup>3,7,8</sup> A possible model to simulate this process is a two-step mechanism: first path (c) occurs; it is followed by the hydrogen migration in the open structure. Since there is retention of the configuration of the N-linked hydrogen during the ring opening leading to structure IV, two hydrogen migration distinct paths are possible. They are represented schematically in Figure 9. In the syn process (path (d)) the migrating hydrogen is cis to the N-linked hydrogen and conversely in the anti process (path (e)) it is trans.

We have adopted for formamide the structure described by Pople et al.<sup>27</sup> in its optimal energy conformation. The first calculated excited states are the  $n\pi^*$  triplet-singlet states. They lie at 5.07 and 5.45 eV above the formamide GS. These values are in good agreement with preceding calculations<sup>28</sup> and experimental results.<sup>29</sup>

For path (d) and path (e), the reaction coordinate is the projection position of the migrating hydrogen on the NC direction. All the other parameters have been optimized all along the process.

In this case, it is difficult to draw a complete MO natural correlation diagram. However we can see that two MOs of

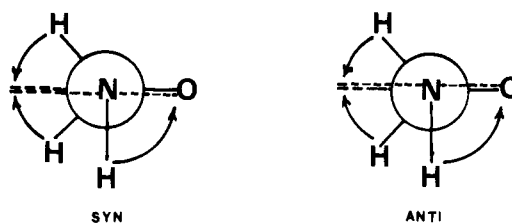


Figure 9. Newman projections of structure IV along the CN bond illustrating the hydrogen motions in paths (d) and (e). The full lines refer to the bond positions in structure IV and the dashed lines to their positions in formamide.

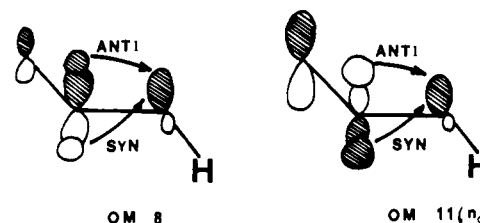


Figure 10. Schematic representation of the occupied MOs 8 and 11 of structure IV mainly concerned in paths (d) and (e). We note that in each case (syn or anti motion), for one MO there is no conservation of the phase properties.

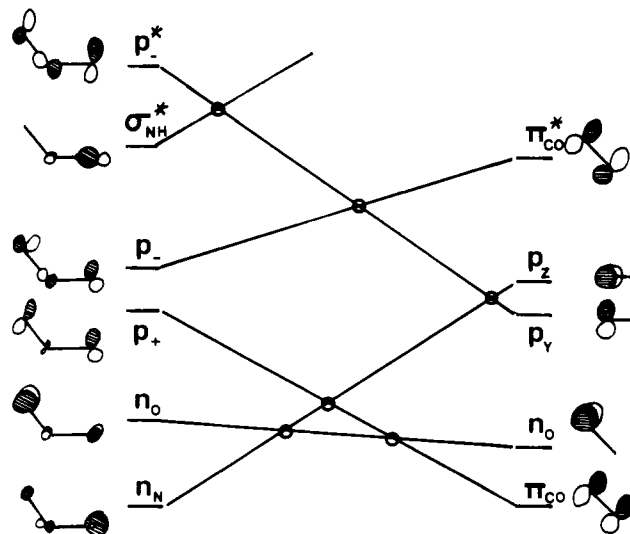


Figure 11. Natural MO correlation diagram in path (f). The circles represent avoided crossings at SCF level.

structure IV are of main concern (see Figure 10). Both are occupied. In one of the syn or anti processes, they would correlate with a formamide occupied MO if the phase continuity is preserved between the C, N, and H lobes when the hydrogen migrates. Now, for the two processes, if one MO satisfies this rule, the other violates it. The consequence is that no clear-cut difference must appear between the  $S_0$  PECs of the two processes.

The calculated PEC corresponding to the syn and anti motions are represented in Figure 8 (right part).<sup>30</sup> They reveal that in the triplet as well in the singlet state the syn process is favored, but that the difference is not significant—i.e., it is less than 0.10 eV. Thus it seems that in substituted compounds the observed migrating aptitude differences are related to bond strength as well as conformational problems rather than to orbital control. The experimental results confirm these findings.<sup>7,8</sup>

**Paths (f) and (g).** From structure IV, another reaction path may be considered. It is the CN bond rupture which leads to formaldehyde and nitrene (path (f)). The CN distance

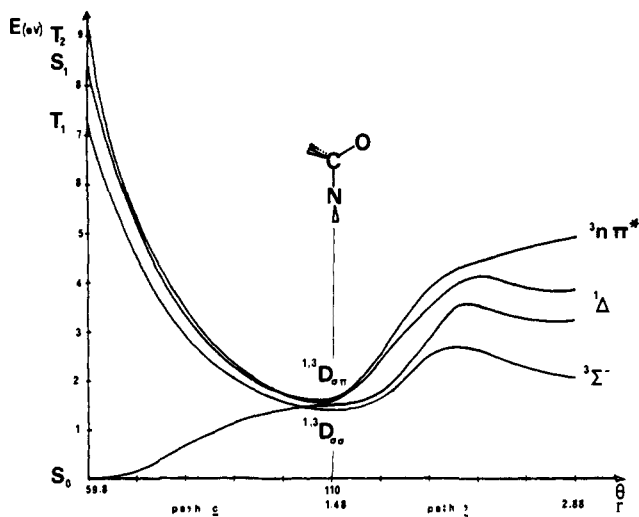


Figure 12. Calculated potential energy curves in path (c) and path (f). The reaction path is related to the formation of nitrene + formaldehyde in a two-step procedure.  $\theta$  refers to the NCO angle and  $r$  to the CN distance.

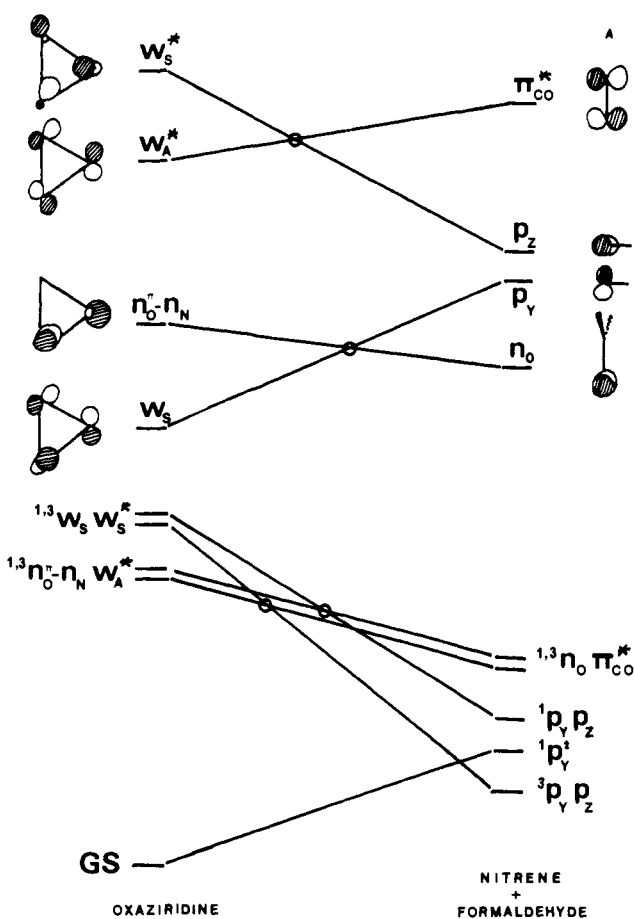


Figure 13. (A) Natural MO correlation diagram in path (g). The circles represent avoided crossings at SCF level. (B) State correlation diagram resulting from the upper natural MO correlations in path (g). The circles represent avoided crossings.

(1.27–2.27 Å) constitutes the reaction coordinate and all the other parameters are linearly varied. The MO natural correlation diagram is shown in Figure 11. There are various crossings, among which is a HOMO–LUMO crossing. They lead to important energy barriers on the first excited state PECs as is confirmed by the calculated ones (Figure 12). Let us note that the calculated  ${}^3\Sigma^-$ – ${}^1\Delta$  separation in nitrene (ca.

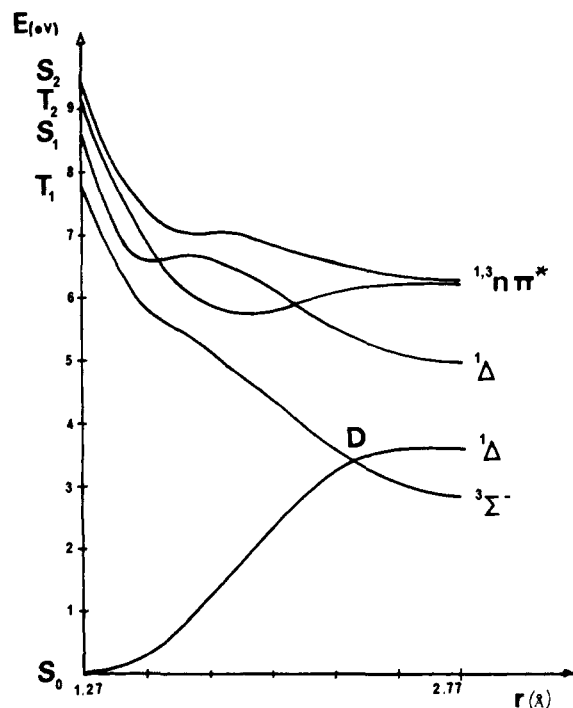


Figure 14. Calculated potential energy curves in path (g). The reaction coordinate is related to the distance between the nitrogen atom and its projection onto the CO bond.

1.5 eV) is in correct agreement with experimental findings.<sup>31</sup>

Thermally, the whole process would need the overcoming of a barrier around 3.8 eV. Photochemically, the process appears to be much easier since the energy requirements are accessible if we consider the internal energy excess resulting from the first step, i.e., path (c).

Another reaction path which leads to the same two products (formaldehyde and nitrene) consists in a synchronous two-bond scission (path (g)). Let us note that the process which does not involve a reorientation of the NH bond is less energetically favorable than the one which requires a progressive reorientation of this bond in the CNO plane.

The MO natural correlation diagram (Figure 13A) shows that no HOMO–LUMO crossing occurs, but that there are crossings between LUMOs on the one hand and between HOMOs on the other hand. The state correlation diagram of Figure 13B results. It shows that there is direct correlation for the  $S_0$  PEC, but that the first excited states are not monotonically correlated. The calculated PECs confirm this analysis (Figure 14).

Thermally, the fragmentation requires a 3.6-eV activation energy, just a little less than in the two-step process. Photochemically, the reaction remains feasible as well in the triplet as in the singlet first excited state, although the existence of some barrier on the corresponding PECs renders it more difficult than the other processes already studied.

In the reverse process—i.e., the addition of nitrene to formaldehyde—the singlet state favors the simultaneous reaction path ( $\geq 0.05$  eV) in comparison with the two-step process (0.3 eV). It is the reverse in the triplet-state reaction. Indeed, in the two-step process, the overcoming of the 0.5-eV energy barrier leads to the formation of the intermediate IV which can easily intersystem cross to the  $S_0$  PEC of oxaziridine. In the simultaneous procedure, the intersystem crossing would occur in an unstable region after overcoming of a 0.8-eV barrier (point D).

## Conclusion

Oxaziridines are such reactive compounds that they were postulated for a long time before being isolated.<sup>3</sup> It was shown that they are closely related to nitrene and formamide isomerization. In particular, recent works report that bicyclic oxaziridines provide a route to synthesize lactams by a stereochemically controlled reaction.<sup>8</sup> It was interesting to try to get theoretical information on this whole pattern. The main results of the present study are the following ones.

The  $S_1$  state of the nitrene leads preferentially to oxaziridine formation through a syn process. It follows that cis nitrene yields cis oxaziridine. The oxaziridine formation would be favored in reducing the  $S_0/S_1$  energy gap in the structure II region. This may be done by stabilizing more  $S_1$  than  $S_0$  in structure II. Nonpolar solvents appear adequate since  $S_0$  has zwitterionic character while  $S_1$  is more diradical. Another possibility is to link electron-withdrawing substituents on the carbon atom—i.e., those which cannot stabilize the main zwitterionic resonant structure of  $S_0$ , but which stabilize  $S_1$ —or on the nitrogen atom—i.e., which lower  $\sigma^+$  and stabilize  $S_1$  more than  $S_0$ .

The  $T_1$  nitrene state yields preferentially cis-trans isomerization.

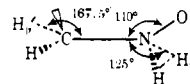
The  $S_1$  state of the oxaziridine leads preferentially to nitrene via a syn process or to formamide via hydrogen migration. The migrating carbon substituent, in the last case, is not determined by orbital factors, but rather by general migrating aptitude, strain energy, and geometrical requirements of the transition state. The nonpolar character of the different transition states of the syn and anti processes invites one to think that the solvent nature is of little effect on the last reaction.

The  $T_1$  state of oxaziridine can also lead to formamide but this is more difficult than in the  $S_1$  state. The same conditions regarding the syn-anti selectivity remain nevertheless. Another reactive path from the same oxaziridine  $T_1$  state is the formation of nitrene but, this time, via an anti motion, contrarily to the  $S_1$  reaction path. An ultimate possibility is the formation of nitrene and formaldehyde in a simultaneous two-bond scission or a two-step procedure. The  $S_1$  state appears much less adequate for these two latter processes than in the preceding ones.

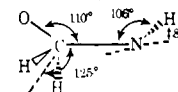
## References and Notes

- For preceding paper see B. Blgot, A. Sevin, and A. Devaquet, *J. Am. Chem. Soc.*, **101**, 1101 (1979).
- This laboratory is associated with CNRS (E.R.A. no. 549).
- W. D. Emmons, *J. Am. Chem. Soc.*, **79**, 5739 (1957).
- (a) J. S. Spiliter and M. Calvin, *J. Org. Chem.*, **23**, 651 (1958); (b) *ibid.*, **30**, 3427 (1965); *Tetrahedron Lett.*, 1445 (1968).
- For a review see C. G. Spence, E. C. Taylor, and O. Buckardt, *Chem. Rev.*, **70**, 231 (1970); A. Padwa, *ibid.*, **77**, 37 (1977).
- F. Krohnke, *Justus Liebigs Ann. Chem.*, **604**, 203 (1957); M. Kamlet and L. Kaplan, *J. Org. Chem.*, **22**, 576 (1957).
- (a) L. S. Kaminsky and M. Lamchen, *J. Chem. Soc.*, C, 2295 (1966); 2128 (1967); (b) R. L. Furey and R. O. Kan, *Tetrahedron*, **24**, 3085 (1965); (c) E. Meyer and G. Griffin, *Angew. Chem., Int. Ed. Engl.*, **6**, 634 (1967); (d) G. F. Field and L. H. Sternback, *J. Org. Chem.*, **33**, 4438 (1968); (e) H. Izawa, P. de Mayo, and T. Tabata, *Can. J. Chem.*, **47**, 51 (1969); (f) M. L. Druelinger, R. W. Shelton, and S. R. Lammert, *J. Heterocycl. Chem.*, **13**, 1001 (1976).
- E. Oliveros-Deshercos, M. Riviere, J. Parelo, and A. Lattes, *Tetrahedron Lett.*, 851 (1975); E. Oliveros, Thesis, University P. Sabatier, Toulouse,

- H. Sugimoto and T. Uschida, *Tetrahedron Lett.*, 2293 (1973); *Bull. Chem. Soc. Jpn.*, **47**, 687 (1974).
- J. B. Bapat and D. St. C. Black, *Chem. Commun.*, 73 (1967); J. S. Spiliter, T. M. Su, H. Ono, and M. Calvin, *J. Am. Chem. Soc.*, **93**, 4075 (1971); D. R. Boyd, W. J. Jennings, and R. Spratt, *Chem. Commun.*, 745 (1970).
- K. Shinzawa and I. Tanaka, *J. Phys. Chem.*, **68**, 1205 (1964); K. Koyano and I. Tanaka, *ibid.*, **69**, 2545 (1965).
- J. Bjorgo and D. R. Boyd, *J. Chem. Soc., Perkin Trans. 2*, 1575 (1973); J. Bjorgo, D. R. Boyd, R. M. Campbell, and N. J. Thomson, *J. Chem. Soc., Chem. Commun.*, 162 (1976).
- N. H. Robb and I. G. Czimadia, *J. Chem. Phys.*, **50**, 1819 (1969).
- (a) A. Devaquet, A. Sevin, and B. Blgot, *J. Am. Chem. Soc.*, **100**, 2009 (1978); B. Blgot, A. Sevin, and A. Devaquet, VII Symposium on Photochemistry, Louvain, 1978; (b) R. B. Woodward and R. Hoffmann, *J. Am. Chem. Soc.*, **87**, 395, 2046 (1965); (c) H. C. Longuet-Higgins and E. Abrahamson, *ibid.*, **87**, 2045 (1965).
- B. Blgot, A. Sevin, and A. Devaquet, *J. Am. Chem. Soc.*, **100**, 2639 (1978).
- W. J. Hehre, W. A. Lathan, R. Ditchfield, M. D. Newton, and J. A. Pople, QCPE No. 236, Indiana University, Bloomington, Ind.
- W. J. Hehre, R. F. Stewart, and J. A. Pople, *J. Chem. Phys.*, **51**, 2657 (1969).
- W. J. Hehre, J. A. Pople, W. A. Lathan, L. Radom, and P. C. Hahiharan, *Top. Curr. Chem.*, **40**, 1 (1973).
- J. Vinh, B. Levy, and P. Millie, *Mol. Phys.*, **21**, 345 (1971), and references cited therein; R. Bonaccorsi, E. Scrocco, and E. Tomasi, *Theor. Chim. Acta*, **21**, 17 (1971).
- The optimized geometry is so defined: CN = 1.33 Å, NO = 1.32 Å, NH = 1.05 Å, CH = 1.09 Å, ONC = 126°, HNC = 115°, NCH<sub>1</sub> = 119.6° NCH<sub>2</sub> = 118.2°.
- P. C. Hiberty and C. Leforestier, *J. Am. Chem. Soc.*, **100**, 2012 (1978).
- T. Kubota and M. Yamakawa, *Bull. Chem. Soc. Jpn.*, **38**, 1552 (1963), and references cited therein.
- (a) This result is in full agreement with preceding reports on the ring opening of three-membered rings: Y. Jean and X. Chapuisat, *J. Am. Chem. Soc.*, **97**, 6325 (1975), and references cited therein; ref 1. (b) This value corresponds to an effective ring opening.
- The optimized structure is so defined: CN = 1.36 Å, NO = 1.36 Å, NH = 1.05 Å, CH = 1.09 Å, ONC = 110°, CNH<sub>1</sub> = 125°, HNH<sub>1</sub> = 73.8°, HCH = 118°, NCH<sub>2</sub> = 167.5°.

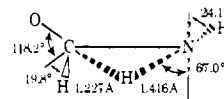


- J. W. Brian, R. D. Boyd, and L. C. Waring, *J. Chem. Soc., Perkin Trans. 2*, 610 (1976).
- R. Hoffmann, *J. Am. Chem. Soc.*, **90**, 1475 (1968).
- The optimized structure of IV is so defined: CN = 1.46 Å, OC = 1.40 Å, NH = 1.05 Å, HCN = 108°, NCH<sub>1</sub> = 125°, CNH = 106°.

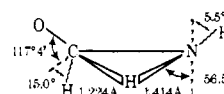


- L. Radom, W. A. Lathan, W. J. Hehre, and J. A. Pople, *Aust. J. Chem.*, **25**, 1601 (1972).
- J. E. Del Bene, G. T. Worth, F. T. Marchese, and M. E. Conrad, *Theor. Chim. Acta*, **36**, 195 (1975); L. Z. Stenkamp and E. R. Davidson, *ibid.*, **44**, 405 (1977).
- G. Herzberg, "Electronic Spectra of Polyatomic Molecules", Van Nostrand, Princeton, N.J., 1967.
- The geometrical parameters defining the transition states of paths (d) and (e) are the following:

path (d): CO = 1.250 Å, CN = 1.435 Å, NCO = 122.2°



path (e): CO = 1.256 Å, CN = 1.432 Å, NCO = 123.0°



- R. S. Berry, "Nitrenes", W. Lwowski, Ed., Interscience, New York, 1970.